Phase Mixing and Island Saturation in Hamiltonian Reconnection

D. Grasso,[1] F. Califano,[1] F. Pegoraro,[1,2] and F. Porcelli[1,3,4]

[1]*Istituto Nazionale Fisica della Materia, Sez. A, Italy*
[2]*Dipartimento di Fisica, Università di Pisa, Italy*
[3]*Dipartimento di Energetica, Politecnico di Torino, Italy*
[4]*Plasma Science and Fusion Center, Massachusetts Institute of Technology, Cambridge, Massachusetts 02139*

(Received 31 July 2000)

The nonlinear evolution of a Hamiltonian magnetic field line reconnection in a two-dimensional fluid plasma leads to a macroscopic equilibrium with a finite-size island and fine-scale spatial structures. The latter arise from the phase mixing of the Lagrangian invariant fields. This equilibrium is the analog of the Bernstein-Greene-Kruskal equilibrium solution for electrostatic Langmuir waves.

DOI: 10.1103/PhysRevLett.86.5051 PACS numbers: 52.35.Py, 47.65.+a, 52.35.Fp, 52.65.Kj

Magnetic field line reconnection in high temperature plasmas is one of the most fertile problems in plasma physics due to its relevance to astrophysical and laboratory plasmas and to its theoretical implications. One of its most important features is the interplay between the energetic and topological aspects that characterize its evolution: a local relaxation of the topological magnetic structure is accompanied by a local, fast release of magnetic energy. The topological features of magnetic reconnection are most evident in the dissipationless (Hamiltonian) regime. In this regime, the topology of the magnetic field is broken by the effect of electron inertia, or by electron kinetic effects not considered in this paper, but the topology of generalized fields is preserved, as discussed in Ref. [1]. While these topological constraints have been shown not to limit the evolution of magnetic reconnection, and in particular the value of the reconnected magnetic flux, their effect on the asymptotic state of the magnetic configuration and on the eventual formation of a "macroscopic" equilibrium has not been fully investigated. In particular the point has been raised that, being collisionless equations reversible, collisionless reconnection may "bounce back," i.e., that, after an initial phase where flux is reconnected, a phase of "unreconnection" may follow, especially if the plasma flow is to decrease as a final steady state is approached.

Nonlinear magnetic reconnection processes due to instabilities have been studied in the collisionless limit in Refs. [1–3]. In Refs. [1,2] a two-dimensional (2D) configuration with double periodic boundary conditions was adopted. With these boundary conditions, an intrinsic limitation is the "cross talking" between island chains when they reach a width comparable to the equilibrium scale length. In this Letter, we remove the double periodic boundary conditions. We adopt a Harris-type equilibrium configuration with a strong superimposed homogeneous magnetic field perpendicular to the reconnection plane. With this configuration, the collisionless evolution of a single coherent magnetic island can be followed until its width saturates at a macroscopic amplitude and its saturation mechanism can be addressed. We find that the saturation mechanism is associated with the energy transport to small scale structures in the fluid vorticity and in the current density inside the island. These structures are superimposed on the macroscopic equilibrium and arise from the phase mixing, inside the island, of the Lagrangian invariants that express the conservation of the topology of the generalized fields. In this way, a new macroscopic equilibrium can be accessed by a Hamiltonian plasma in spite of energy conservation.

We consider a 2D configuration with a strong magnetic field in the ignorable z direction, $\mathbf{B} = B_0\mathbf{e}_z + \nabla\psi \times \mathbf{e}_z$, where B_0 is constant and $\psi(x, y, t)$ is the magnetic flux function. The governing equations, normalized on the Alfvén time τ_A and on the equilibrium scale length L_{eq}, can be cast in the Lagrangian invariant form [4]

$$\frac{\partial G_\pm}{\partial t} + [\phi_\pm, G_\pm] = 0\,, \tag{1}$$

with Hamiltonian $H = -\int d^2x\,(\phi_+ G_+ + \phi_- G_-)/2$. Here, $[A, B] = \mathbf{e}_z \cdot \nabla A \times \nabla B$, and the Lagrangian invariants are

$$G_\pm \equiv \psi - d_e^2\nabla^2\psi \pm d_e\varrho_s\nabla^2\varphi\,. \tag{2}$$

These conserved fields are advected along the stream lines of

$$\phi_\pm \equiv \varphi \pm (\varrho_s/d_e)\psi\,. \tag{3}$$

The magnetic flux ψ and the plasma stream function φ obey the equations

$$\psi - d_e^2\nabla^2\psi = (G_+ + G_-)/2\,, \tag{4}$$

$$d_e\varrho_s\nabla^2\varphi = (G_+ - G_-)/2\,, \tag{5}$$

with d_e the electron collisionless skin depth and ϱ_s the so-called ion sound gyro radius. The more standard form of the reduced two-fluid equations can be found, e.g., in Refs. [1,4–6]. In particular, $J = -\nabla^2\psi$ is the current density, $U = \nabla^2\varphi$ is the plasma fluid vorticity along z, and the generalized Ohm's law is

$$\frac{\partial F}{\partial t} + [\varphi, F] = \eta(J - J_0) + \varrho_s^2[U, \psi]\,, \tag{6}$$

with $F \equiv \psi - d_e^2\nabla^2\psi$ the generalized magnetic flux and η the electrical resistivity, which is set to zero in the Hamiltonian limit.

The initial equilibrium $\mathbf{B}_{\rm eq} = B_0\mathbf{e}_z + \mathbf{B}_{y\rm eq}(x)\mathbf{e}_y$, where $\mathbf{B}_{y\rm eq}(x) = \tanh(x)$, is unstable to tearing perturbations periodic in y over the distance L_y when $1 < \pi L_y$.

In the x direction we impose the perturbed fields $\delta\psi$ and $\delta\varphi$ to vanish at infinity. The model is solved numerically on a limited integration domain along x such that the boundary fluxes are negligible, using a nonuniform mesh with an increasing density of points in the central region. A suitable filtering [7] of the small spatial scales (well below the electron skin depth) has been included, which is capable of ensuring numerical stability, while not altering the requested conservation properties significantly. This method is more convenient than artificial viscosity or hyperviscosity, which require smaller values of the time step for numerical stability and, in the time asymptotic limit, also affect the larger scales. The model preserves parity, so we choose initial perturbations such that $\psi(-x) = \psi(x)$ and $\varphi(-x) = -\varphi(x)$. These relations imply $H = 0$ and $G_+(-x, y) = G_-(x, y)$, $\phi_+(-x, y) = -\phi_-(x, y)$.

As we anticipated, the functions $G_\pm$ develop fine-scale oscillations due to phase mixing. This process can be conveniently interpreted in terms of a formal analogy with the standard Vlasov-Poisson problem for electrostatic Langmuir waves [8]. The set in Eq. (1) has the form of two coupled 1D Vlasov equations, with x and y playing the roles of the coordinate and of the conjugate momentum for the "distribution functions" $G_\pm$ of two "particle" species with opposite charges in the Poisson-type equation for φ, Eq. (5), and equal charges in the Yukawa-type equation for ψ, Eq. (4). The stream functions $\phi_\pm$ play the role of the single particle Hamiltonians. Thus, similar to Bernstein-Greene-Kruskal (BGK) [9] solutions, the stationary solutions of Eq. (1) can be written in the form $G_\pm = \mathcal{G}(\pm\phi_\pm)$. Note that there is a single function $\mathcal{G}$ because of the symmetry condition. However, the present problem and the standard Vlasov-Poisson problem are not formally identical. In Poisson's equation, the source term is the electron density, which is the velocity space integral of the distribution function and as such does not exhibit fine-scale oscillations. In our problem, the source terms for Eqs. (4) and (5) are the distribution functions $G_\pm$ themselves. However, the field ψ and φ solutions of these equations can be expressed in terms of integrals of $G_\pm$. Thus, the fine-scale structure of the $G_\pm$ does not show up in ψ and φ. A similar situation arises also in the case of the diocotron instability in magnetized, non-neutral plasmas [10]. There, the electron density, which is the source term in Poisson's equation, is a Lagrangian invariant and thus exhibits phase mixing.

Now, we show the results of the numerical integration of Eq. (1) for $L_y = 4\pi$, which implies that the standard parameter Δ' related to the logarithmic derivative of the linear eigenfunction for the perturbed magnetic flux outside the reconnection layer has a value $\Delta' = 15.7$. Furthermore, we choose an integration domain that extends from $-L_x$ to L_x with $L_x = 12.35$ and $d_e = \varrho_s = 0.2$. For comparison, we also consider a case with $d_e = 0$ and $\varrho_s = 0.1$ in which resistivity replaces inertia in the generalized Ohm's law and take $(\eta)^{1/3} = 0.2$. With these parameters, the corresponding regime is the "large Δ' limit" [2], where the nonlinear reconnection process is fast. In the collisionless regime, the initial nonlinear growth is superexponential in time, as already found in Refs. [1–3] and shown here in Fig. 1. The magnetic island reaches a macroscopic width over a time scale of the order of the inverse linear growth rate, γ_L. In the collisional case the growth rate is lower but the saturation level is comparable for the two cases.

The numerical approach is limited by the necessity of a finite-size grid, which we control by the use of filters. As a consequence, the filamentary structures generated by the phase mixing are smoothed out as soon as they reach the grid scale length. In order to check that such numerical "coarse graining" on the grid size does not influence the large scale structures, as well as the characteristic time of the process, we have performed a number of simulations with varying spatial grid sizes which show that the filaments just persist for a longer time at higher resolution without significantly changing the larger scale dynamics. When the action of the filter starts to influence the energy balance, the simulation is terminated.

We see in Fig. 2a that the magnetic energy $\int d^2x\,|\nabla\psi|^2$ is transformed mainly into ion (plasma) kinetic energy, $\int d^2x\,|\nabla\varphi|^2$, into electron parallel kinetic energy, $\int d^2x\,d_e^2J^2$, and into electron internal energy, $\int d^2x\,\varrho_s^2U^2$. The total energy $\mathcal{E}$ is defined as

$$\mathcal{E} \equiv \int d^2x\,(|\nabla\psi|^2 + d_e^2J^2 + \varrho_s^2U^2 + |\nabla\varphi|^2)/2\,, \quad (7)$$

where the difference between $\mathcal{E}$ and the Hamiltonian H is a (conserved) quadratic functional of the Lagrangian invariants $G_\pm$ [4].

In the initial equilibrium configuration, the contour levels of the Lagrangian invariants $G_\pm$ are simply $y = \text{const}$ lines. As the instability evolves, these lines are transported along the characteristic curves, $x_\pm(t)$, determined by

$$d\vec{x}_\pm(t)/dt = \vec{v}_\pm(\vec{x}_\pm, t), \quad \text{with } \vec{v}_\pm = \vec{e}_z \times \nabla\phi_\pm\,. \quad (8)$$

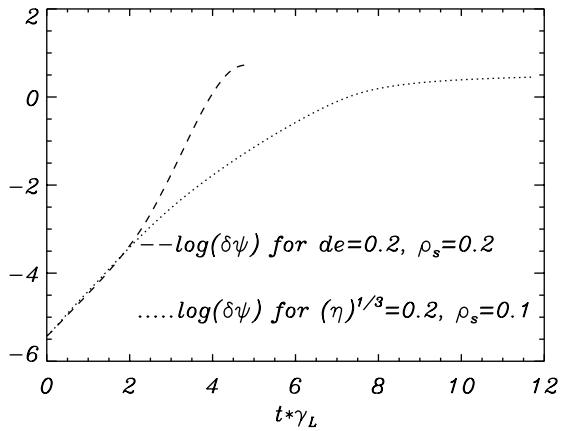

FIG. 1. Growth rate: $\ln(\delta\psi_X)$ versus the normalized time $t\gamma_L$ for the collisionless and the resistive case, with $\gamma_L = 0.028$ and $\gamma_L = 0.025$, respectively.

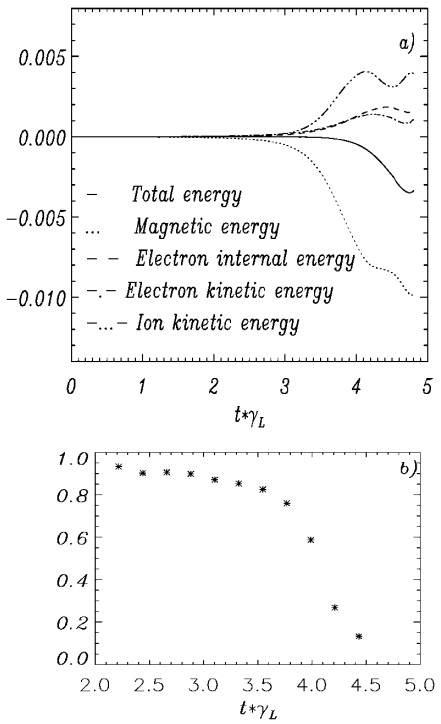

FIG. 2. (a) The difference between each term of energy, as defined in Eq. (7), and the correspondent value at $t = 0$, divided by the total energy $\mathcal{E}(0)$, is plotted versus the normalized time $t * \gamma_L$. (b) Plot of $\int dx\, dy\, (\langle\langle[\phi_\pm, G_\pm]\rangle\rangle)^2 / \int dx\, dy\, ([\phi_\pm, G_\pm])^2$ versus time, where $\langle\langle\cdots\rangle\rangle$ denotes spatial averaging over $2d_e$, for a case with $d_e = 0.2$, $\varrho_S = d_e/2$. All the integrals are extended over the entire slab.

Therefore, two vortical patterns (one the mirror image of the other) develop inside the island location. The advection of $G_\pm$ along these vortices leads to the phase mixing of the two Lagrangian invariants. An equivalent view is that the single particle Hamiltonians $\phi_\pm$ develop two separatrices and that fluid elements advected by the velocity fields $\vec{v}_\pm$ become trapped inside these separatrices in the x, y phase space as shown in Fig. 3. The phase mixing of $G_\pm$ is also responsible for the formation of the typical "quadrupolar" fine spatial structures, with odd symmetry for the plasma vorticity $U = (G_+ - G_-)/(2\rho_s d_e)$ and even symmetry for the generalized flux function $F = (G_+ + G_-)/2$. This quadrupolar structure is also clearly visible in the contour plot of the stream function φ shown in Fig. 4a in comparison with the collisional case (Fig. 4b). We see that, in the collisionless case, convection cells appear inside the magnetic island, around the O points of the magnetic flux. Here we choose a time in which the magnetic island has an amplitude of order 3.7. As the island grows, new cells appear. At saturation the velocity field is completely localized inside the magnetic island and tends to vanish outside. By contrast, in the resistive case, the velocity field tends to be more widely distributed.

A new characteristic dynamical time related to the eddy turn-over time inside the island becomes of interest. This time scale becomes shorter as the instability grows and can be estimated to be inversely proportional to the square root of the amplitude of the perturbed fields. When the turning time becomes of the order of the nonlinear island growth time, energy is removed effectively from the large spatial scales leading to the island growth saturation.

In order to show that this process can allow the plasma to access a new "macroscopic" stationary state, we proceed along lines that are similar to those followed in Ref. [11] for the BGK solutions in the case of the nonlinear Landau damping of Langmuir waves. We separate the Lagrangian invariants into coarse-grained and phase-mixed parts according to $G_\pm = \bar{G}_\pm + \tilde{G}_\pm$. Then, the numerical

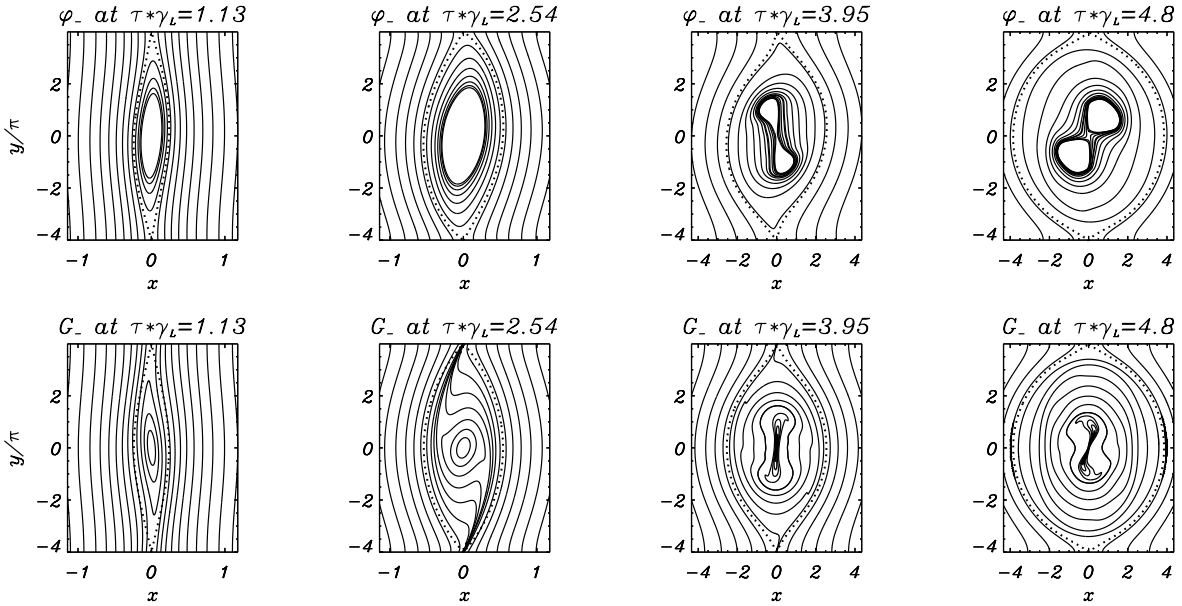

FIG. 3. The contour levels of the single particle Hamiltonian φ_- at different simulation times are plotted in the first row. The dotted lines are the separatrices. The contour levels of the Lagrangian invariant G_- are drawn in the second row (the dotted contour is the island separatrix). Note that the scale in the x direction changes during time. All the plots refer to a simulation with $d_e = \varrho_s = 0.2$.

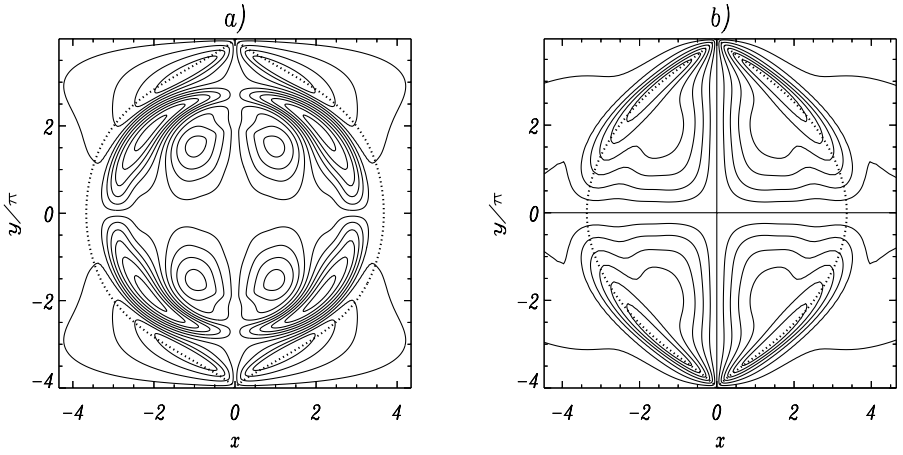

FIG. 4. Stream function φ for the collisionless and resistive case, at a time such that the amplitude of the magnetic island (dotted contour) is comparable and of order 3.7 for case (a) and 3.3 for case (b). (a) collisionless case with $d_e = \varrho_s = 0.2$; (b) resistive case with $d_e = 0.2, \varrho_s = 0.1$.

solutions of Eqs. (4) and (5) show that, when the turning time is shorter than the growth time, $\varphi \approx \bar{\varphi}$ and $\psi \approx \bar{\psi}$, since the contributions of the phase-mixed parts, $\tilde{G}_\pm$, are averaged out. On the other hand, these parts continue to contribute to total energy conservation through the $d_e^2 J^2$ and the $\varrho_s^2 U^2$ terms in Eq. (7). This makes it possible for the coarse-grained quantities to reach a macroscopic equilibrium given by $[\bar{\varphi}_\pm, \bar{G}_\pm] \to 0$ without violating energy conservation, consistent with the plot in Fig. 2b, which shows that the integral of the squared coarse-grained Poisson brackets in Eq. (1) decays in time (the nonsquared quantity gives trivially a zero integral). Together with the symmetry conditions, $[\bar{\varphi}_\pm, \bar{G}_\pm] \to 0$ gives

$$\bar{\psi} - d_e^2 \nabla^2 \bar{\psi} \pm d_e \varrho_s \nabla^2 \bar{\varphi} = \mathcal{G}[\bar{\psi} \pm (d_e/\varrho_s)\bar{\varphi}]. \qquad (9)$$

We assume, consistently with the numerical results, that $\bar{\psi}$ is the dominant term on the left-hand side of Eq. (9). In particular, at saturation, $\nabla^2 \bar{\psi} \sim \psi$ and $\bar{\varphi} \sim d_e^2 \bar{\psi}$ [we assume for simplicity that $\varrho_s/d_e \approx O(1)$]. Then, the arbitrary function $\mathcal{G}$ must be of the form $\mathcal{G}(A) \approx A + d_e^2 \mathcal{F}(A)$, where $\mathcal{F}(A) = O(A)$ and d_e^2 plays the role of the smallness parameter. Thus, by expanding Eq. (9), we obtain

$$-d_e^2 \nabla^2 \bar{\psi} \pm d_e \varrho_s \nabla^2 \bar{\varphi} = \pm (d_e/\varrho_s)\bar{\varphi} + d_e^2 \mathcal{F}(\bar{\psi}). \qquad (10)$$

This equation contains odd and even terms. Balancing the even terms gives $\bar{J} = \mathcal{F}(\bar{\psi})$. The odd terms imply $\varrho_s^2 \nabla^2 \bar{\varphi} \sim \bar{\varphi}$ and therefore $\max(\bar{U}) \sim \max(\bar{J})$, which is also confirmed by the numerical results. The functional dependence of $\bar{J}$ on $\bar{\psi}$ is not determined by Eq. (9) and should be obtained from the nonlinear evolution of the instability. It is remarkable, however, that the function $\mathcal{F}$ need not contain either d_e or ϱ_s, which may explain why the saturated island width is found to be comparable in both collisionless and resistive regimes (cf. Fig. 1).

We have investigated the nonlinear evolution of fast magnetic reconnection in the collisionless regime, all the way to saturation, and the establishment of a new equilibrium with a macroscopic magnetic island. This new equilibrium is accessed in spite of energy conservation. Part of the released magnetic energy is transferred to small scale structures for the conserved fields, which are averaged out in the expression for the magnetic flux function. This result uncovers the underlying unity between different physical phenomena, such as nonlinear Landau damping of Langmuir waves [11] and dissipationless vortex interaction [12] in 2D fluids on one side and Hamiltonian magnetic field line reconnection on the other.

This work was supported in part by the Italian National Research Council (CNR) and by MURST.

[1] E. Cafaro *et al.*, Phys. Rev. Lett. **80**, 4430 (1998); D. Grasso *et al.*, Plasma Phys. Controlled Fusion **41**, 1497 (1999).
[2] M. Ottaviani and F. Porcelli, Phys. Rev. Lett. **71**, 3802 (1993).
[3] A. Aydemir, Phys. Fluids B **4**, 3469 (1992); R. G. Kleva *et al.*, Phys. Plasmas **2**, 23 (1995); X. Wang and A. Bhattacharjee, Phys. Rev. Lett. **70**, 1627 (1993).
[4] B. N. Kuvshinov *et al.*, J. Plasma Phys. **59**, 727 (1998).
[5] T. Schep *et al.*, Phys. Plasmas **1**, 2843 (1994).
[6] B. N. Kuvshinov *et al.*, Phys. Lett. A **191**, 296 (1994).
[7] S. K. Lele, J. Comput. Phys. **103**, 16 (1992).
[8] T. O'Neil, Phys. Fluids **8**, 2255 (1965).
[9] I. B. Bernstein, J. M. Greene, and M. D. Kruskal, Phys. Rev. **108**, 546 (1957).
[10] R. C. Davidson, *An Introduction to the Physics of Nonneutral Plasmas* (Addison-Wesley, Reading, MA, 1990).
[11] C. Lancellotti and J. J. Dorning, Phys. Rev. Lett. **81**, 5137 (1998); G. Manfredi, Phys. Rev. Lett. **79**, 2815 (1997); M. Brunetti, F. Califano, and F. Pegoraro, Phys. Rev. E **62**, 4109 (2000).
[12] J. Miller, P. B. Weichman, and M. C. Cross, Phys. Rev. A **45**, 2328 (1992).